Adaptive nonlinear observer for electropneumatic clutch actuator with position sensor

Hege Langjord*, Glenn-Ole Kaasa** and Tor Arne Johansen*

***Abstract*—This paper proposes an adaptive nonlinear observer for an electropneumatic clutch actuator. Estimates of piston velocity, chamber pressures and dynamic friction state are made based on piston position measurement only. Parameter estimations of the clutch load characteristics and friction coefficients are treated through adaptation, and the persistence of excitation conditions for convergence of the estimation errors are derived. The performance of the adaptive observer is evaluated and is compared to experimental measurements obtained in a test truck.**

I. Introduction

The electropneumatic actuator considered in this paper is applied to automate the clutch actuation in manual transmission, for Automated Manual Transmissions (AMT), or Clutch-By-Wire (CBW) applications for heavy duty trucks. AMT systems have seen a growth in popularity, especially in the European market [1], over the last decade as they can easily be added on to existing Manual Transmission (MT) systems.

Primarily for cost reasons, pneumatics are preferred in our case, as pressurized air is already present in trucks. Pneumatic actuators are common as industrial actuators, [2]. This is due to their desired properties, especially clean operations, low cost, high force-to-mass ratio, and easy maintenance. Control design for such actuators have received a lot of research interest, both for systems with proportional valves [3]-[5] and with on/off solenoid valves [6]-[8] for the control of flow to the actuator. The main drawback compared to hydraulic actuators, is their inherently nonlinear behavior, mainly arising from compressibility of air, stiction and high friction forces.

Cost is a crucial factor in the automotive industry, and it is desired to reduce the number of sensors to a minimum. The clutch actuator system considered provides measurements of the piston position only. For nonlinear control of the actuator, [9], [10], and [11], real-time information of velocity and the pressure in the actuator chamber are also needed, hence estimation of these states must be obtained. In addition, accurate estimation of the friction and the clutch load characteristics are important since they have a major influence on the clutch actuator dynamics, and performance of model-based state feedback control design suffer due to model errors as demonstrated in [12]. Off-line estimation of the clutch load characteristic was treated in [13], but since both the load and friction forces change during operation, slow but persistent adaptation of the load characteristic and friction coefficients are desired to obtain satisfactory accuracy in the the pressure estimates.

General designs for nonlinear observers have been developed for particular classes of pneumatic actuators. Wu et al., [14], considered nonlinear observability analysis for a pneumatic actuator systems, and concluded that in general it is not feasible to guarantee a convergent pressure estimate from measurements of position only. Therefore, observers presented for pneumatic actuator systems are designed and analysed specifically. Bigras and Khayati, [15], presented a nonlinear observer for estimation of the pressure in a pneumatic cylinder, ensuring exponential stability of the estimation error. Pandian et al. [16] proposed a Luenberger-type observer and a sliding mode observer to estimate pressure in a cylinder actuator, and Gulati and Barth, [17] presented two Lyapunov-based pressure observers for a pneumatic actuator system. In our clutch actuator system, the clutch load is a position dependent and time-varying load while observers in the above references treat electropneumatic actuators with constant loads. Some load independent and varying load observers can be found, Taghizadeh et al. [18] designed a Kalman filter to observe velocity for a pneumatic actuator with varying load, while Gulati and Barth [19] presented an energy-based observer which is load-independent. But as [18] only consider a velocity observer, while [19] use both position and velocity measurement and focus only on pressure estimation, these observers are not applicable to our system. In addition [15]-[19] all use simpler friction model than required in our system, and has no adaptation to capture a time-varying clutch load. From experimental testing it is clear that the clutch actuator also has hysteresis, and we account for this in the friction modeling which contains dynamic friction. The theses by Kaasa [20] and Vallevik [21] considered observer designs for the same clutch actuator system as ours, but without rigorously deriving sufficient conditions for the convergence of estimation errors. These authors also consider a three-way proportional valve as the control valve while we consider on/off-solenoid valves. The only other work on observers for electropneumatic clutch system actuated by on/off solenoid valves found in the literature is [22] which proposed a feedback linearization-based observer, but did not consider adaptation.

This paper proposes an adaptive nonlinear observer which is a deterministic observer with linear output-injections and adaptation laws for load characteristics and friction, where the state errors converge to zero under persistence of excitation (PE) conditions. It is derived using standard control Lyapunov design principles [23]. While [20] includes test rig experiments, the present paper uses production quality sensors installed in a test truck. These are more influenced by noise and vibrations that must be accounted for in the design. No other adaptive observer with derived sufficient conditions for convergence of the estimation errors is found in literature for systems like the considered clutch actuator system. This would be systems that are characterized by strongly uncertainties and time-varying clutch load characteristic, strong dynamic friction

*{hegesan,torj}@itk.ntnu.no, Department of Engineering Cybernetics, NTNU, Trondheim, Norway.

**gkaa@statoil.com, Statoil Research Centre, Porsgrunn, Norway

and with only position sensor available. The design of an adaptive observer is important as it is intended for the dual mode switched controller with state feedback [11].

A preliminary reduced-order observer is presented in [24], while the present paper contributes with an extended full order observer with noise filtering and an experimental comparison that shows its benefits.

The remainder of the paper is organized as follows. We present the clutch actuator and its model in Section 2. Section 3 proposes an adaptive nonlinear full-order observer that ensures convergence of the estimation errors. The results from experiments are presented in Section 4. Section 5 gives the conclusions.

II. Model of the clutch actuator

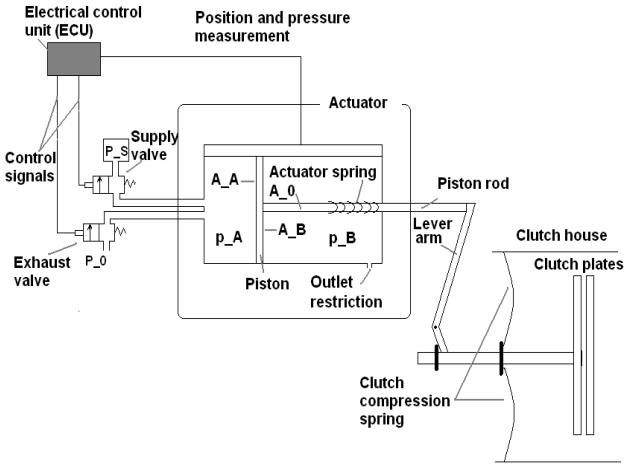

Fig. 1. A schematic of the clutch actuator system with actuator, valves, sensor, clutch and ECU.

Figure 1 presents a schematic of the considered clutch actuator system. The electronic control unit (ECU) calculates and sends control signals to the supply and exhaust valves. These valves control the resulting flow into/out of the actuator chamber, respectively. The piston acts on the clutch through the piston rod. At the zero piston position the clutch plates are engaged and as the piston moves to the right (air added to the actuator) the clutch plates are pulled apart, first they will be slipping and then fully disengaged. The motion of the piston is given by Newton's 2nd law of motion, as a result of the spring forces, the friction and the pressure forces,

$$\begin{aligned} M\dot{v} &= -f_l(y) - f_f(v,z) + \frac{A_A R T_0}{V_A(y)} m_A \\ &\quad - \frac{A_B R T_0}{V_B(y)} m_B - A_0 P_0. \end{aligned} \tag{1}$$

The parameters and variables are given in Table I and the model terms are further described below. $V_A(y) = V_{A,0} + A_A y$ and $V_B(y) = V_{B,0} - A_B y$ describe the chamber volumes, and m_A and m_B describe the mass of air in the chambers related

TABLE I
Parameters and variables for the clutch actuator model

y	Piston position
v	Piston velocity
$\frac{F}{K_z} z$	Pre-sliding deflection (friction state)
p_A, p_B	Pressure in chambers A,B
m_A, m_B	Mass of air in chambers A,B
u	Normalized control input to valve set
A_A, A_B	Area of chambers A,B
A_0	Area of piston rod
P_0	Ambient pressure
P_S	Supply pressure
D	Viscous damping coefficient
K_z	Deflection stiffness coefficient
F	Coulomb friction coefficient
T_0	Ambient temperature
R	Gas constant of air
M	Mass of piston
$V_{A,0}, V_{B,0}$	Volume of chambers A,B at $y = 0$
R_0, R_1	Valve opening constants
ρ_0	Density of air
C	Capacity

to the corresponding chamber volume and pressures according to

$$p_A(p_A, y) = \frac{RT_0}{V_A(y)} m_A \tag{2}$$

$$p_B(p_B, y) = \frac{RT_0}{V_B(y)} m_B, \tag{3}$$

where the simplifying assumption of constant air temperature T_0 has been made as the pressure dynamics sensitivity to temperature changes is found to be small in practice [20]. Due to wear, the characteristics of the clutch compression spring may change, and the clutch load force, $f_l(y)$, which is the lumped force of this spring and the counteracting, much weaker, actuator spring, changes accordingly. The force increases with wear, especially for lower piston positions. It can be parametrized in the affine form

$$f_l(y) = \phi^T(y)\,\theta \tag{4}$$

where $\phi(y)$ is a vector of basis functions and θ is the corresponding weighting parameter vector. To obtain a model with few parameters, the two B-splines shown in Figure 2(a) are used as basis functions $\phi(y) = (\phi_1(y), \phi_2(y))^T$, see Appendix A for more details. The resulting load force is shown in Figure 2(b) with $k = [0, 0.5, 8]$ and $\theta = [4, 5]$, together with an estimated clutch load characteristic obtained from pressure measurement as $A_A(p_A - P_0)$, derived from motion dynamics by assuming $v = 0$ and $p_B = P_0$.

The friction acting on the piston is modeled by a viscous damping term with parameter D and a Coulomb friction term with parameter F,

$$f_f(v,z) = Dv + Fz \tag{5}$$

The friction dynamics are modeled by a simplified LuGre model [20],

$$\frac{F}{K_z}\dot{z} = v - |v|\, z \tag{6}$$

where $\frac{F}{K_z} z$ is the normalized pre-sliding deflection state.

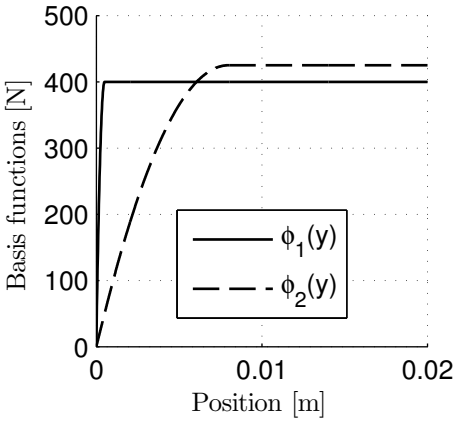

(a) The basis functions used for clutch load modeling.

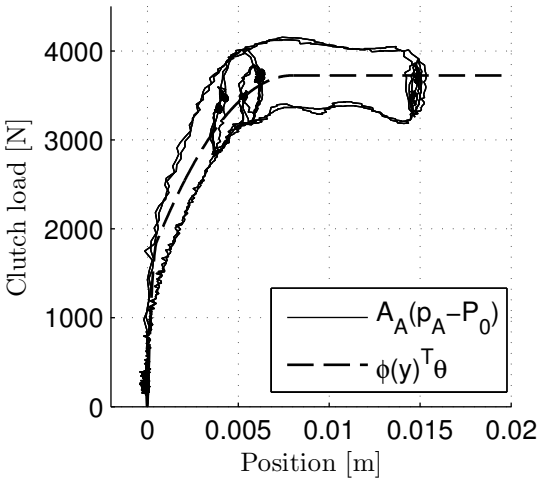

(b) Clutch load, modeled (dashed) and experimental (dashed). The experimental data $A_A(p_A - P_0)$ includes not only the clutch load force but also the effect of dynamic friction (hysteresis).

Fig. 2. Clutch load characteristics and model with two B-spline basis functions.

Mass balances for chambers A and B are

$$\dot{m}_A = w_v(p_A, u) \tag{7}$$
$$\dot{m}_B = w_r(p_B) \tag{8}$$

To describe the flow w_v through the control valves of chamber A, and the flow w_r through the outlet restriction of chamber B, we use a simplified version of the standardized orifice flow equation, [25], (see also [20])

$$w = \rho_0 C \omega(r) p_h \tag{9}$$

where $r = \frac{p_l}{p_h}$ and the pressure ratio function $\omega(r)$ is

$$\omega(r) = \begin{cases} \sqrt{1-r^2}, & r \in [0,1] \\ 0, & r > 1. \end{cases} \tag{10}$$

The air flow to chamber A can be expressed as

$$w_v(p_A, u) = w_{c,supp} y_{u,supp} - w_{c,ex} y_{u,ex} \tag{11}$$

where

$$y_{u,supp} = sat_{[0,1]}\left(\frac{1}{R_1 - R_0}(u_{supp} - R_0)\right) \tag{12}$$
$$y_{u,ex} = sat_{[0,1]}\left(\frac{1}{R_1 - R_0}(u_{ex} - R_0)\right) \tag{13}$$

describes the mean valve opening where u_{supp} and u_{ex} are the command inputs of the valves PWM input, R_0 is the command input where the valve starts to open and R_1 is the command input where the valve is fully opened. $w_{c,supp}$ and $w_{c,ex}$ are given by (9)-(10) according to Table II. The flow of chamber B is

$$w_r(p_B) = w_{in} - w_{out}, \tag{14}$$

where w_{in} represents the flow through the outlet restriction if $P_0 > p_B$ and w_{out} represents the same flow if $p_B > P_0$ given by (9)-(10) according to Table II. These flow functions are easily shown to satisfy

$$\frac{\partial w_v}{\partial p_A}(p_A, u) \le 0, \quad \forall p_A \in [P_0, P_S], \forall u \in [0,1] \tag{15}$$
$$\frac{\partial w_r}{\partial p_B}(p_B) < 0, \quad \forall p_B \in [0, \infty\rangle. \tag{16}$$

which will be instrumental in the analysis and design of the nonlinear observer.

TABLE II
HIGH AND LOW PRESSURES FOR THE FLOWS THROUGH THE ON/OFF SOLENOID VALVES, AND THE FLOW THROUGH THE OUTLET RESTRICTION, RESPECTIVELY, USED IN (11) AND (14)

Flow	p_l	p_h
$w_{c,supp}$	p_A	P_S
$w_{c,ex}$	P_0	p_A
w_{in}	p_B	P_0
w_{out}	P_0	p_B

In summary, this gives the 5th order model

$$\dot{y} = v \tag{17a}$$
$$M\dot{v} = -f_l(y) - f_f(v,z) + \frac{A_A R T_0}{V_A(y)} m_A - \frac{A_B R T_0}{V_B(y)} m_B - A_0 P_0 \tag{17b}$$
$$\frac{F}{K_z}\dot{z} = v - |v| z \tag{17c}$$
$$\dot{m}_A = w_v(p_A, u) \tag{17d}$$
$$\dot{m}_B = w_r(p_B). \tag{17e}$$

III. ADAPTIVE NONLINEAR OBSERVER

Only position measurement is available in the production system, and for control purposes [9]-[11] we need estimates of pressure of chamber A and velocity. The proposed observer also provides estimates of the other states, the pressure in chamber B and pre-sliding deflection. This is only used for improving the model to get more accurate estimates of p_A and v, but are in themselves not important.

Due to temperature changes and wear, the friction and clutch load characteristics change during the operation and lifetime of the clutch. Therefore, adaptation of the load and

friction characteristics are desired in order to achieve sufficient accuracy of the observer, and we propose adaptation laws for the clutch load parameters, θ, and the viscous damping, D. Adaptation of the Coulomb friction, F, has been considered too, but has been left out as it enters nonlinearly into the friction dynamics and an adaptive law is harder to design. It is also found that sufficient accuracy can be obtained without estimating F and no significant improvement is achieved by estimating F.

To account for the clutch load curve moving significantly to the left/right (see Figure 2) due to wear and temperature changes, a Multiple Model Scheme can be used, where a supervisory logic chooses the best set of basis functions from multiple models with ϕ_2 deflecting at different positions similar to [26], [27].

We propose the full-order observer

$$\begin{aligned}
\dot{\hat{y}} &= \hat{v} + l_y(y-\hat{y}) && (18a)\\
M\dot{\hat{v}} &= -\phi^T(\hat{y})\hat{\theta} - \hat{D}\hat{v} - F\hat{z} + \frac{A_A RT_0}{V_A(y)}\hat{m}_A && (18b)\\
&\quad -\frac{A_B RT_0}{V_B(y)}\hat{m}_B - A_0P_0 + l_v(\dot{y}-\hat{v})\\
\frac{F}{K_z}\dot{\hat{z}} &= \hat{v} - |\dot{y}|\hat{z} && (18c)\\
\dot{\hat{m}}_A &= w_v(\hat{p}_A, u) + \frac{l_m}{V_A(y)}(\dot{y}-\hat{v}) && (18d)\\
\dot{\hat{m}}_B &= w_r(\hat{p}_B), && (18e)
\end{aligned}$$

where $l_y, l_v, l_m \geq 0$ are observer injection gains and the adaptation laws for $\hat{\theta}$ and $\hat{D}$ are

$$\dot{\hat{\theta}} = -\Gamma\phi^T(\hat{y})(\dot{y}-\hat{v}) \quad (19)$$

$$\dot{\hat{D}} = -\gamma_D\hat{v}(\dot{y}-\hat{v}) \quad (20)$$

with the gain matrix $\Gamma = \Gamma^T > 0$ and $\gamma_D > 0$. As seen in the proof below, the adaptation laws (19)-(20) result from a Lyapunov design and the assumptions $\dot{\theta} = 0$ and $\dot{D} = 0$.

Introducing $\dot{y}$ in the observer design requires careful attention, as differentiation of the measured signal will amplify any measurement noise. Note that the injection terms $l(\dot{y}-\hat{v})$ are implementable with only y measured, *i.e.* without using $\dot{y}$ explicitly, see Appendix B. The effects of measurement noise will be discussed later when considering experimental results.

The error dynamics are given by

$$\begin{aligned}
\dot{\tilde{y}} &= \tilde{v} - l_y\tilde{y} && (21a)\\
M\dot{\tilde{v}} &= -\phi^T(y)\theta + \phi^T(\hat{y})\hat{\theta} - (D+l_v)\tilde{v} && (21b)\\
&\quad -\tilde{D}\hat{v} - F\tilde{z} + \frac{A_A RT_0}{V_A(y)}\tilde{m}_A - \frac{A_B RT_0}{V_B(y)}\tilde{m}_B\\
\frac{F}{K_z}\dot{\tilde{z}} &= \tilde{v} - |v|\tilde{z} && (21c)\\
\dot{\tilde{m}}_A &= -a(t)\tilde{m}_A - \frac{l_m}{V_A(y)}\tilde{v} && (21d)\\
\dot{\tilde{m}}_B &= -b(t)\tilde{m}_B && (21e)\\
\dot{\tilde{\theta}} &= \Gamma\phi^T(\hat{y})\tilde{v} && (21f)\\
\dot{\tilde{D}} &= \gamma_D\hat{v}\tilde{v} && (21g)
\end{aligned}$$

where we get from (15)-(16) and the mean value theorem that

$$a(t) = -\frac{\partial w_v(\bar{m}_A, u)}{\partial p_A} \geq 0 \quad (22)$$

$$b(t) = -\frac{\partial w_r(\bar{m}_B)}{\partial p_B} \geq b_0 > 0 \quad (23)$$

and

$$\begin{aligned}
\bar{m}_A &\in [\min(m_A, \hat{m}_A), \max(m_A, \hat{m}_A)]\\
&\subseteq \left[\frac{V_{A\min}}{RT_0}P_0, \frac{V_{A\max}}{RT_0}P_S\right] && (24)\\
\bar{m}_B &\in [\min(m_B, \hat{m}_B), \max(m_B, \hat{m}_B)]\\
&\subseteq [0, \infty\rangle && (25)
\end{aligned}$$

where $V_{A,\min} = V_A(0)$ and $V_{A,\max} = \inf_y V_A(y)$.

Proposition 1. *The observer presented in (18) with the adaptation laws (19) and (20), where $l_v, l_m \geq 0$, $l_y > \frac{(\alpha + K\theta_{\max})^2}{2\alpha l_v}$, $\alpha > 0$ and $\Gamma = \Gamma^T > 0, \gamma_D > 0$, ensures that for any physically meaningful initial conditions and system trajectories*

1) *the error dynamics (21) are stable and all estimates are bounded*
2) *$\tilde{v}$, $\tilde{m}_B$ and $\tilde{y}$ converge to zero*
3) *if v and u are persistently exciting (PE) then also $\tilde{m}_A$ and $\tilde{z}$ converge to zero*

Proof: Stability of the error dynamics can be established using the Lyapunov function candidate

$$\begin{aligned}
V =& \frac{\alpha}{2}\tilde{y}^2 + \frac{M}{2}\tilde{v}^2 + \frac{F^2}{2K_z}\tilde{z}^2 + \frac{1}{2}\Gamma^{-1}\tilde{\theta}^T\tilde{\theta} + \frac{1}{2\gamma_D}\tilde{D}^2 \quad (26)\\
&+ \frac{A_A RT_0}{2l_m}\tilde{m}_A^2 + \frac{1}{2Db_0}\left(\frac{A_B RT_0}{V_{B\min}}\right)^2\tilde{m}_B^2,
\end{aligned}$$

where $\inf_y V_B(y) = V_{B\min}$. The time-derivative of V along the trajectories of the error dynamics are

$$\begin{aligned}
\dot{V} &= \alpha\tilde{y}\tilde{v} - \alpha l_y\tilde{y}^2 - \phi^T(y)\theta\tilde{v} + \phi^T(\hat{y})\theta\tilde{v}\\
&\quad -(D+l_v)\tilde{v}^2 - F|v|\tilde{z}^2 - \frac{A_A RT_0}{l_m}a(t)\tilde{m}_A^2\\
&\quad -\frac{A_B RT_0}{V_B(y)}\tilde{v}\tilde{m}_B - \frac{b(t)}{Db_0}\left(\frac{A_B RT_0}{V_{B\min}}\right)^2\tilde{m}_B^2.
\end{aligned}$$

The Mean Value Theorem gives

$$|\phi^T(y) - \phi^T(\hat{y})| \leq K|\tilde{y}| \quad (27)$$

where $K = \max_{\bar{y}}\left\|\frac{\partial\phi(\bar{y})}{\partial y}\right\|$. Using this, $\theta_{max} = \|\theta\|$ and (23), we see that $\dot{V}$ satisfies

$$\begin{aligned}
\dot{V} \leq& \alpha\tilde{y}\tilde{v} - \alpha l_y\tilde{y}^2 + \theta_{max}K|\tilde{y}\tilde{v}|\\
&-(D+l_v)\tilde{v}^2 - F|v|\tilde{z}^2 + \frac{A_B RT_0}{V_{B\min}}|\tilde{v}\tilde{m}_B| \quad (28)\\
&-\frac{1}{D}\left(\frac{A_B RT_0}{V_{B\min}}\right)^2\tilde{m}_B^2 - \frac{A_A RT_0}{l_m}a(t)\tilde{m}_A^2.
\end{aligned}$$

Using Young's inequality

$$xy \leq \frac{x^2}{2\varepsilon} + \frac{\varepsilon y^2}{2}$$

with

$$\varepsilon_1 = \frac{A_B RT_0}{DV_{B\min}},$$

and

$$\varepsilon_2 = \frac{K\theta_{max} + \alpha}{l_v},$$

we obtain

$$\frac{A_B R T_0}{V_{B\min}} |\tilde{v}\tilde{m}_B| \leq \frac{D}{2}\tilde{v}^2 + \frac{1}{2D}\left(\frac{A_B R T_0}{V_{B\min}}\right)^2 \tilde{m}_B^2$$

and

$$(K\theta_{max} + \alpha)|\tilde{y}\tilde{v}| \leq \frac{l_v}{2}\tilde{v}^2 + \frac{(K\theta_{max} + \alpha)^2}{2l_v}\tilde{y}^2.$$

This gives

$$\dot{V} \leq -\frac{D + l_v}{2}\tilde{v}^2 - F|v|\tilde{z}^2 - \frac{1}{2D}\left(\frac{A_B R T_0}{V_{Bmin}}\right)\tilde{m}_B^2 \qquad (29)$$
$$-\frac{A_A R T_0}{l_m} a(t)\,\tilde{m}_A^2 - \left(-\frac{(K\theta_{max} + \alpha)^2}{l_v} + \alpha l_y\right)\tilde{y}^2.$$

Since

$$l_y > \frac{(\alpha + K\theta_{max})^2}{2\alpha l_v} \qquad (30)$$

this proves stability of the error dynamics. Barbalat's lemma [23] gives that $\tilde{y}$, $\tilde{v}$ and $\tilde{m}_B$ converge to zero for any trajectories. With PE of v it follows by standard arguments that $\dot{V}$ will be negative definite also in $\tilde{z}$, which implies that $\tilde{z}$ also converges to zero. PE of u gives $\int_t^{t+T} a(\tau)d\tau > 0$ and implies that also $\tilde{m}_A$ converges to zero.

IV. Experimental results

The nonlinear observer is implemented in a dSPACE rapid prototyping system and Simulink by using explicit Euler discretization. The Euler integration step size is set to 0.1 ms and the measurement sampling rate in the experiments is also 1 ms. Measurements from experiments conducted in a test truck at Kongsberg Automotive ASA are used to test the observer. Figure 3 shows the reference clutch sequence used in these experiments and Table III presents the characteristics of the on/off valveset used in the experiments. These experiments also provide measurements of the pressure in chamber A, and these are used for verifying the observer performance only. The measurements are obtained with production quality sensors, and the measurements suffer from noise and vibrations.

TABLE III
Supply and exhaust valve characteristics

Opening time	0.5 ms
Closing time	2.5 ms
Maximum volumetric flow rate, supply	14 l/s
Maximum volumetric flow rate, exhaust	16 l/s

Figure 4 shows the results with the adaptive observer. The tuning parameters are given in Table IV. The start values of the parameter estimates have been set far from the expected values to test the performance of the adaptation laws. Results from the two initial conditions 1) $\theta_0 = [10, 10]$, $D_0 = 50$ and 2) $\theta_0 = [1, 1]$, $D_0 = 5000$ are included in Figures 5 and 6 to show convergence of the estimated parameters. Note that

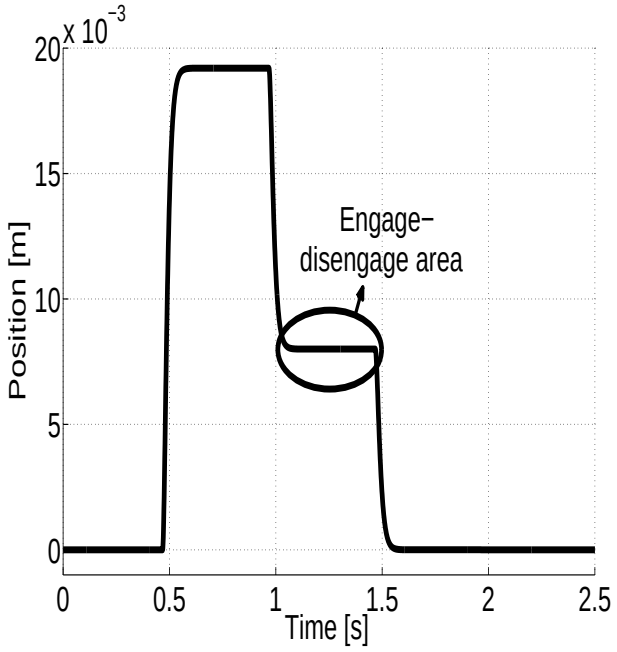

Fig. 3. Reference clutch sequence used in the experiments.

such large changes in friction and clutch load characteristics as used for testing here will not occur rapidly during the normal operation of the clutch system. During normal operation the unknown parameters are expected to be slowly time-varying parameters which adaptive observers in practice should able to track. We have used slow adaptation of the clutch load, as it is expected to improve the robustness of the approach. The gain Γ is set 30 times higher in the region $3 - 6$ mm as the clutch load characteristics are especially important in this area due to the steep curve, and since this region is visited only for short transient periods with a typical clutch sequence. The adaptation is shut down whenever the position is not changing, due to lack of PE that might lead to drift or divergence of the estimates. The estimate of the pressure in chamber A improves over time and we have a good estimate after approximately 150 s corresponding to adaptation in about 60 clutch sequences as seen from Figure 4. From Figure 6 it is clear that the adaptation of θ gives an accurate estimate of the clutch load characteristic. This indicates that the clutch sequence in Figure 3 provides sufficient excitation to estimate both load and friction coefficients simultaneously. In some cases, such as a cold start of the truck, faster adaptation is needed due to large temperature gradients. This is possible if the clutch is used sufficiently and the piston position reference is changed often enough, i.e. PE of u and v is provided, something which usually will be done when starting to drive. The adaptation gains can also be increased for the first 10-20 gear shifts after a cold start, but care must be taken since tests with higher gains show that although convergence speed increases significantly and stable estimates are achieved, the estimates tend to vary more after convergence.

A reduced order adaptive observer was proposed and tested in [24], where results of similar accuracy were shown for

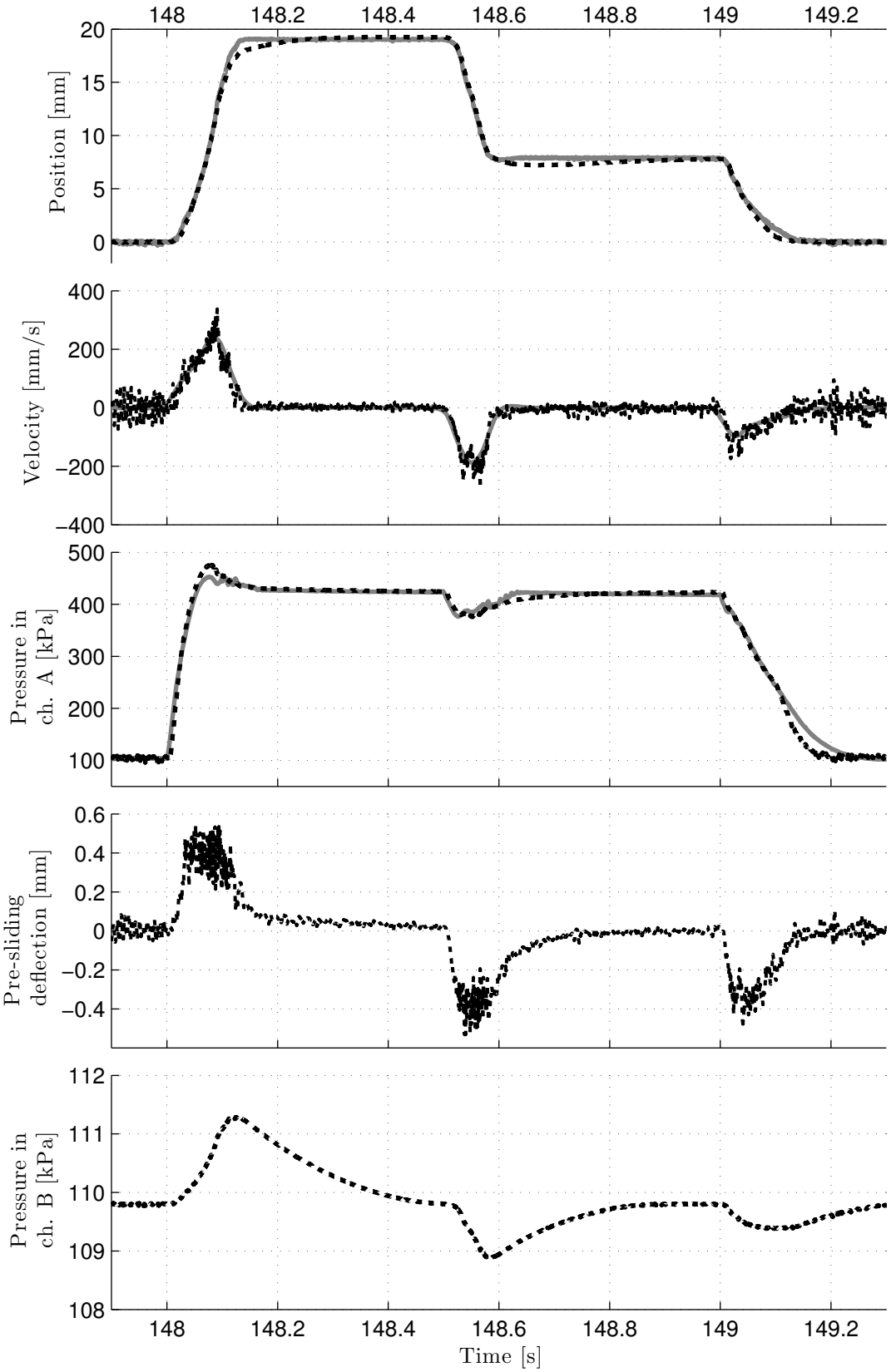

Fig. 4. Experiments with full order nonlinear observer with adaptation of θ and D. The curves show estimates after $t = 148\ s$ where the parameter adaptation has already converged, after about 60 clutch sequences. Observer states are dashed, and measurements from the truck are shown in solid gray. For velocity, the measurement curve is filtered from position measurement.

TABLE IV
OBSERVER INJECTION GAINS

Parameter	Value
l_y	10
l_v	2000
l_m	10^{-5}
Γ	$I \cdot 0.1$
γ_D	$4 \cdot 10^5$

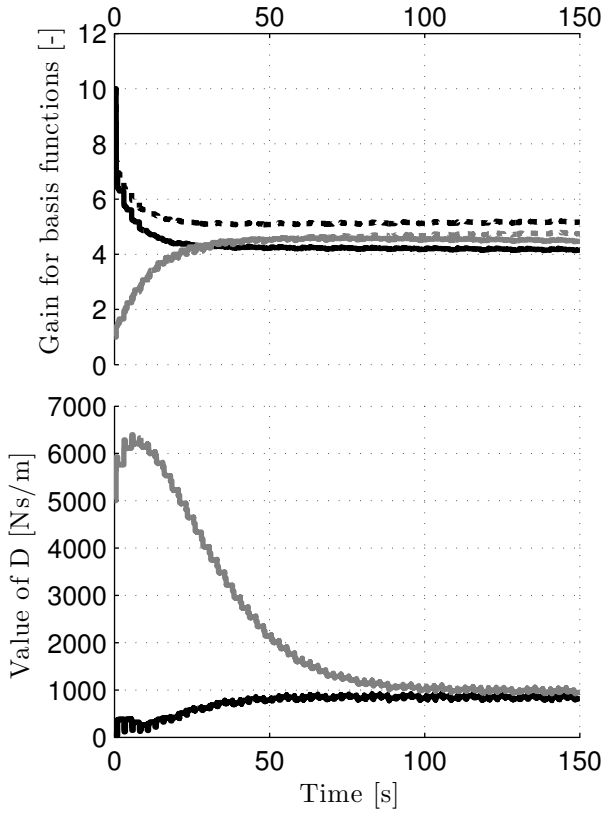

Fig. 5. Estimated parameters during 150 s where 60 clutch sequences are executed. Results for $\theta_0 = [10, 10]$, $D_0 = 50$ are shown in black and for $\theta_0 = [1, 1]$, $D_0 = 5000$ in gray. θ_1 are shown dotted and θ_2 are shown solid in the upper plot.

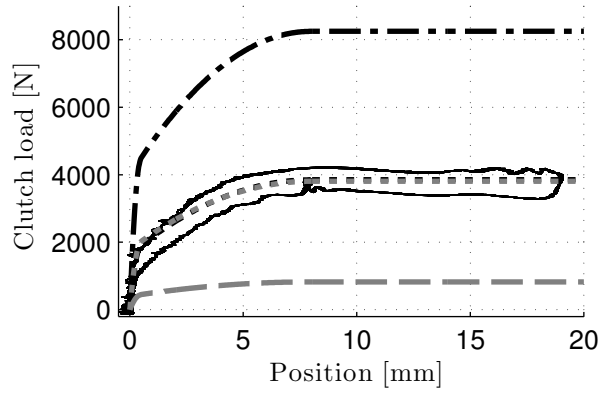

Fig. 6. Clutch load characteristics, estimated through $A_A(p_A - P_0)$ solid, dot dashed in black for $\theta_0 = [10, 10]$, $D_0 = 50$ and dashed in gray for $\theta_0 = [1, 1]$, $D_0 = 5000$, while the curves with the estimated $\hat{\theta}$ at $t = 150$ are dotted in black and gray respectively.

the estimated pressure in chamber A, while velocity and friction suffer from much higher noise levels. Table V lists the average and maximum absolute errors for the estimates of the pressure in chamber A, and it is clear that the full-order observer improves the pressure estimate since the effect of noise is reduced. Preliminary simulation testing of the adaptive observer combined with the dual-mode switched controller derived in [11] indicates that the noise level present in the observer is of a magnitude which is acceptable for control purposes [28] .

TABLE V
MAXIMUM AND AVERAGE ERROR FOR PRESSURE OF CHAMBER A FOR FULL- AND REDUCED ORDER ADAPTIVE OBSERVERS, CALCULATED IN THE TIME INTERVAL $140 \leq t \leq 150$

Adaptive observer	Maximum pressure error	Average pressure error
Full-order	45.01 kPa	6.01 kPa
Reduced-order [24]	75.86 kPa	8.44 kPa

V. CONCLUSIONS

A nonlinear observer for an electropneumatic clutch actuator has been presented, and adaptation laws for clutch load characteristics and viscous friction force are given. The estimation errors are shown to be convergent under PE conditions. Performance of both the nonlinear observers and the parameter estimations are studied and validated compared to experimental results from a test truck, and good results are shown compared to the reduced order adaptive observer [24].

Acknowledgments: This work has been sponsored by the Research Council of Norway and Kongsberg Automotive ASA.

APPENDIX A
LOAD CHARACTERISTICS

These spline basis functions are built up by polynomials

$$\phi_1(x) = \begin{cases} 0, & x < k_1 \\ a_1 x^2 + b_1 x, & k_1 \leq x < k_2 \\ a_1 k_2^2 + b_1 k_2, & x \geq k_2 \end{cases}$$

$$\phi_2(x) = \begin{cases} 0, & x < k_1 \\ 10^5 (x - k_1), & k_1 \leq x < k_2 \\ a_2 x^2 + b_2 x + c_2, & k_2 \leq x < k_3 \\ a_2 k_3^2 + b_2 k_3 + c_2 & x \geq k_3 \end{cases}$$

To be able to find the spline coefficients from the positions of the knots, k, we need specific criteria.

- ϕ_1
  - Derivative in k_2 is to be equal to zero
  - The value is to be 400 in k_2
- ϕ_2 :
  - Transition between the linear and the quadratic part is to be smooth
  - Derivative in k_2 is to be equal to one
  - Derivative in k_3 is to be equal to zero

Mathematically, this gives us

$$\xi_i = A_i^{-1} B_i \qquad i = 1, 2$$

where

$$A_1 = \begin{bmatrix} k_2^2 & k_2 \\ 2k_2 & 1 \end{bmatrix} A_2 = \begin{bmatrix} k_2^2 & k_2 & 1 \\ 2k_2 & 1 & 0 \\ 2k_3 & 1 & 0 \end{bmatrix}$$

$$\begin{aligned} B_1 &= [400, 0]^T \\ B_2 &= \left[10^5(k_2 - k_1), 10^5, 0\right]^T \end{aligned}$$

and

$$\begin{aligned} \xi_1 &= [a_1, b_1]^T \\ \xi_2 &= [a_2, b_2, c_2]^T \end{aligned}$$

APPENDIX B
IMPLEMENTATION OF $\dot{y}$

We demonstrate how $\dot{y}$ can be implemented without using the differentiate signal by looking at the velocity dynamics, where u_v contains the remaining terms from (18c)

$$M\dot{\hat{v}} = u_v + l_v\left(\dot{y} - \hat{v}\right).$$

Integration gives

$$\begin{aligned} M\hat{v} &= \int_0^t \left(u_v + l_v\left(\frac{dy}{d\tau} - \hat{v}\right)\right) d\tau \\ &= \int_0^t \left(u_v - l_v\hat{v}\right) d\tau + l_v \int_{y(0)}^{y(t)} dy \\ &= \int_0^t \left(u_v - l_v\hat{v}\right) d\tau + l_v\left(y\left(t\right) - y\left(0\right)\right). \end{aligned}$$

the estimate $\hat{v}$ can be implemented without differentiation as

$$\begin{aligned} \dot{x_v} &= u_v - l_v\hat{v} \\ M\hat{v} &= x_v + l_v(y - y(0)). \end{aligned}$$

The term $\int_0^t f(t_k)\frac{dy(t_k)}{dt_k}d\tau$, with $f(t_k) = \frac{F}{F_C}\hat{z}_k, -\Gamma\phi^T(\hat{y}_k), -\gamma_D\hat{v}_k$ respectively, which appears for the estimates of z, θ and D can be implemented in discrete-time in the case of using zero-order hold on the measurements, which we usually have, and simple Euler integration as $f(t_{k-1})(y(t_k) - y(t_{k-1})$.

REFERENCES

[1] L. Glielmo, L. Iannelli, V. Vacca, and F. Vasca, "Gearshift control for automated manual transmissions," *IEEE/ASME Transactions on Mechatronics*, vol. 11, pp. 17–26, 2006.

[2] M. Smaoui, X. Brun, and D. Thomasset, "A combined first and second order sliding mode approach for position and pressure control of an electropneumatic system," in *Proceedings of the American Control Conference*, Portland, 2005.

[3] Z. Rao and G. M. Bone, "Nonlinear modelling and control of servo pneumatic actuators," *IEEE Transaction on Control System Technology*, vol. 16, pp. 562–569, 2008.

[4] A. Girin, F. Plestana, X. Brun, and A. Glumineau, "High-order sliding-mode controllers of an electropneumatic actuator: Application to a aeronautic benchmark," *IEEE Transactions on Control System Technology*, vol. 17, no. 3, pp. 663–645, 2009.

[5] E. Richer and Y. Hurmuzlu, "A high performance pneumatic force actuator system: Part ii-nonlinear control design," *Journal of Dynamic Systems, Measurement and Control*, vol. 122, pp. 426–434, 2000.

[6] A. K. Paul, J. K. Mishra, and M. G. Radke, "Reduced order sliding mode control for pneumatic actuator," *IEEE Transactions on Control Systems Technology*, vol. 2, pp. 271–276, 1994.

[7] K. Ahn and S. Yokota, "Intelligent switching control of pneumatic actuator using on/off solenoid valves," *Mechatronics*, vol. 15, pp. 683–702, 2005.

[8] T. Nguyen, J. Leavitt, F. Jabbari, and J. E. Bobrow, "Accurate sliding-mode control of pneumatic systems using low-cost solenoid valves," *IEEE/ASME Transactions on Mechatronics*, vol. 12, pp. 216–219, 2007.

[9] H. Sande, T. A. Johansen, G. O. Kaasa, S. R. Snare, and C. Bratli, "Switched backstepping control of an electropneumatic clutch actuator using on/off valves," in *Proceedings of the 26th American Control Conference*, New York, 2007, pp. 76–81.

[10] H. Langjord, T. A. Johansen, and J. P. Hespanha, "Switched control of an electropneumatic clutch actuator using on/off valves," in *Proceedings of the 27th American Control Conference*, Seattle, WA, 2008.

[11] H. Langjord and T. A. Johansen, "Dual-mode switched control of an electropneumatic clutch actuator," *IEEE/ASME Transaction on Mechatronics, DOI: 10.1109/TMECH.2009.2036172*, vol. (In Press), 2010.

[12] H. Langjord, T. A. Johansen, and C. Bratli, "Dual-mode switched control of an electropneumatic clutch actuator with input restrictions," in *Proceedings of the European Control Conference*, Budapest, Hungary, 2009.

[13] H. Langjord, T. A. Johansen, S. R. Snare, and C. Bratli, "Estimation of electropneumatic clutch actuator load characteristics," in *Proceedings of the 17th IFAC World Congress*, Seoul, Korea, 2008.

[14] J. Wu, M. Goldfarb, and E. Barth, "On the observability of pressure in a pneumatic servo actuator," *Journal of Dynamic Systems, Measurement, and Control*, vol. 126, pp. 921–924, 2004.

[15] P. Bigras and K. Khayati, "Nonlinear observer for pneumatic system with non negligble connection port restriction," in *Proceedings of the 21th American Control Conference*, Anchorage, AK, 2002.

[16] S. R. Pandian, F. Takemura, Y. Hayakawa, and S. Kawamura, "Pressure observer-controller design for pneumatic cylinder actuators," *IEEE/ASME Transaction on Mechatronics*, vol. 7, pp. 490–499, 2002.

[17] N. Gulati and E. J. Barth, "Non-linear pressure observer design for pneumatic actuators," in *Proceedings of the 2005 IEEE/ASME International Conference on Advanced Intelligent Mechatronics*, Monterey, CA, 2005.

[18] M. Taghizadeh, F. Najafi, and A. Ghaffari, "Multimodel pd-control of a pneumatic actuator under variable loads," *International Journal of Advanced Manufacturing Technology*, vol. 48, pp. 665–662, 2010.

[19] N. Gulati and E. J. Barth, "A globally stable load-independent pressure observer for the servo control of pneumatic actuators," *IEEE/ASME Transactions on Mechatronics*, vol. 14, pp. 295–306, 2009.

[20] G. O. Kaasa, "Nonlinear output-feedback control applied to electropneumatic clutch actuation in heavy-duty trucks," Ph.D. dissertation, Norwegian Univeristy of Science and Technology, 2006.

[21] G. Vallevik, "Adaptive nonlinear observer for electropneumatic clutch actuation," Master's thesis, Norwegian Univeristy of Science and Technology, 2006.

[22] T. Szabo, M. Buckholz, and K. Dietmayer, "A feedback linearization based observer for an electropneumatic clutch actuated by on/off solenoid valves," in *Proceedings of the 2010 IEEE Multi-conference on Systems and Control*, Yokahama, Japan, 2010.

[23] H. K. Khalil, *Nonlinear Systems*, 3rd edition, Ed. Prentice Hall, Upper Saddle River, New Jersey, 2000.

[24] H. Langjord, G. O. Kaasa, and T. A. Johansen, "Nonlinear observer and parameter estimation for electropneumatic clutch actuator," in *Proceedings of the 8th IFAC Symposium on Nonlinear Control Systems*, Bologna, Italy, 2010.

[25] I. ISO, "ISO 6358 - pneumatic fluid power - components using compressible fluids - determination of flow-rate characterictics," ISO-Int. Organization for Standardization, Tech. Rep. 1st edition, 1989.

[26] J. Bakkeheim and T. A. Johansen, "Transient performance, estimatior resetting and filtering innonlinear multiple model adaptive backstepping control," *IEE Proceedings - Control Theory & Applications*, vol. 153, pp. 536–545, 2006.

[27] K. S. Narendra and K. George, "Adaptive control of simple nonlinear systems using multiple models," in *Proceedings of the 21th American Control Conference*, Anchorage, AK, 2002, pp. 1779–1784.

[28] H. Langjord, G. O. Kaasa, and T. A. Johansen, "Adaptive observer-based switched controller for electropneumatic clutch actuator with position sensor," in *Submitted to: IFAC World Congress*, Milan, Italy, 2011.